Ab Initio Study of the Torsional Spectrum of Glycolaldehyde

M. L. Senent*

Departamento de Astrofisica Molecular e Infrarroja, Instituto de Estructura de la Materia, C.S.I.C., Serrano 113b, Madrid 28006, Spain

Received: March 11, 2004; In Final Form: June 3, 2004

The torsional spectrum of glycolaldehyde ($COH-CH_2OH$) is predicted from MP4(SDTQ)/cc-pVQZ ab initio calculations. This monosaccharide of astrophysical interest shows two large amplitude vibrations that confer nonrigid properties: the central bond torsion and the OH torsion. It presents five stable conformers, three of C_s symmetry (I-cis, II-trans, and IV-cis) and a double minimum of C_1 symmetry (III-trans and III′-trans). The favorite geometry, I-cis, stabilizes by the formation of a hydrogen bond connecting the eclipsed oxygen atoms. The relative energies of the secondary minima are 1278.2 (II-trans), 1297.2 (III and III′-trans) and 1865.2 cm^{-1} (IV-cis). A barrier of 1895 cm^{-1} hinders the cis → trans interconversion. The barriers for the OH torsion are 2040 (cis) and 191 and 713 cm^{-1} (trans). The torsional energy levels have been calculated variationally up to $J = 6$ using a flexible model in two dimensions. Far-infrared frequencies and intensities have been determined at room temperature. In addition, the rotational parameters of the I-cis conformer have been computed to be $A = 18\,583.85$ MHz, $B = 6563.83$ MHz, $C = 5009.34$ MHz, $D_J = -20.18$ kHz, $D_{JK} = -82.36$ kHz, and $D_K = 138.38$ kHz at the zero vibrational level. The parameters corresponding to the trans form are $A = 38\,019.19$ MHz, $B = 4406.79$ MHz, $C = 4076.73$ MHz, and $D_J = -109.28$ kHz.

Introduction

Glycolaldehyde is the first monosaccharide detected in the interstellar medium (ISM).[1] It represents a well-known molecule atmospherically relevant[2] and a potential intermediary in the prebiotic syntheses of sugars.

The impact of the detection has been significant although its abundance in the ISM is very low. It accomplishes the set of $C_2O_4H_2$ isomers discovered, which has increased the interest in the study of isomerism in interstellar chemistry.[1] Characteristic millimeter-wave rotational transitions have been observed in emission toward Sagittarius B2 (N) (SgrB2(N)) with the National Radio Astronomy Observatory (NRAO) 12-m.[1] Later investigations have confirmed its insignificant abundance in other sources.[3] Recently, Hollis et al.[4] have spatially mapped the galactic center SgrB2(N) for evaluating the abundance ratio of the detected isomers (glycolaldehyde/acetic acid/methyl formate = 0.5:1:26).

Ab initio calculations can help the search for solutions of many astrophysical problems. Organic species such as glycolaldehyde bring up new questions to the astronomers related to the chemical evolution of the ISM and the interpretation of the observed spectra. Their mechanisms of formation in the ISM at low temperatures are the subject of recent investigations that suggest models in gas and in solid phase.[5−7] The radiative association reactions in gas phase proposed by Huntress and Mitchell for methyl formate[5] seem not to be able to be extended to all the observed large molecules. Because they become visible on surfaces, it is generally accepted that the surface of the interstellar dust grains plays an important role.[7] It may be assumed that molecular groups forming these species were synthesized on the grains and afterward the molecules were deposited in the gas phase.

Even though many mechanisms of glycolaldehyde formation occur in gas phase at low pressures and temperatures, few experimental[8−12] and theoretical[13−15] data are available for the isolated species. Databases for astrophysical molecules[12] simply collect the rotational parameters and the dipole moments of refs 8, 9, and 11 for the cis conformer. For this reason, the main goal of this paper is to obtain as much information as possible related to structural and spectroscopic properties that can be derived from ab initio calculations. Previous and extensive experience in ab initio studies of nonrigid molecules can help in elucidating the results without the use of experimental data for evaluating calculations.[16−25]

It may be expected that from the astrophysical point of view the large amplitude vibrations of glycolaldehyde will be the most interesting internal motions because they produce the nonrigidity and involve low energy levels that can be populated at very low temperatures. The low-frequency modes are the torsion of the central bond and the torsion of the hydroxyl alcoholic group. The first motion transforms the cis conformer, the one that has been detected, into an undetected trans minimum related to a secondary minimum conformation. Theoretically, it has been demonstrated that the cis form is the most stable geometry due to the formation of an intramolecular hydrogen bond.[15] However, to my knowledge, there are not available data for the trans form that is supposed to be less abundant. Marstokk and Møllendal,[8−9] who have measure the microwave spectrum of a mixture at room temperature, have assigned more than 90% of the lines to the cis conformer and have evaluated the dipole moment.

There are not astrophysical traces of *trans*-glycolaldehyde. Perhaps, it does not exist in the interstellar medium, or perhaps, its abundance with respect to the cis form is very low. It has to be taken into consideration that *cis*-glycolaldehyde is already a molecule of very low abundance. Then, the object of this paper is to use the ab initio calculations for determining the relative stabilities and the sizes of the torsional barriers that hinder the internal rotation. If these barriers are high enough and the

* E-mail address: imts420@iem.cfmac.csic.es.

10.1021/jp0489121 CCC: $27.50
Published on Web 07/02/2004

formation mechanisms in the grains can produce both conformers, both geometries can coexist at low temperatures. It is well-known that conformers of ethanol, a nonrigid molecule of similar properties, coexist in glass phases.[26]

Few experimental spectroscopic properties corresponding to *cis*-glycolaldehyde are published. To my knowledge, the far-infrared region has not been explored. Previous works are from Niki et al.,[10] who have detected the molecule among the products in photolysis of C_2H_4 + NO in air using the long-path Fourier transform infrared spectroscopy (FTIR) method, and from Butler et al.,[11] who have measured recently the millimeter- and submillimeter-wave spectrum. They provide the rotational parameters of the cis form ground state. Niki et al.[10] have assigned nine vibrational bands of the absorption spectrum recorded between 600 and 2000 cm^{-1} and 2500 and 3700 cm^{-1}.

Without experimental measurements for evaluating the current results, this paper represents a prediction of properties unable to be compared with experimental data. For example, the far-infrared spectrum, which provides the most important information about torsional transitions, is not available. The plausibility of the results is based on a large amount of previous works where the model has been tested. Former investigations of molecules with internal rotation have demonstrated that the torsional barriers and fundamental frequencies for large amplitude motions can be calculated accurately using Möller−Plesset theory and extended basis sets, if the geometry is allowed to be relaxed. For example, the single-rotor torsional barriers of acetone,[16] dimethyl ether,[17] hydrogen peroxide,[21] ethanol,[22] and acetic acid[23] have been determined to be 267.1, 950.6, 406.1, 1296.3, and 169.8 cm^{-1}, close to the experimental values of 266.1, 942.6, 387.1, 1251, and 168.2 cm^{-1} [see refs 16, 17, and 21−23]. In the cases of molecules with two strongly interacting rotors, these parameters are effective barriers defined in one-dimension after one of the rotating groups is frozen at its minimum energy position.

Methods, Discussion, and Conclusions

Computational Details. The potential energy surface of glycolaldehyde has been determined with MP4(SDTQ)/cc-pVQZ ab initio calculations. The geometries of all the conformations have been optimized at the MP2/cc-pVQZ level. All the calculations have been performed with Gaussian 98.[27]

The harmonic frequencies corresponding to the conformers have been computed at the MP2/cc-pVTZ level using the method implemented in Gaussian 98.[27] The torsional levels have been calculated variationally with a flexible two-dimensional model depending on the two torsional angles. The kinetic energy parameters of the Hamiltonian have been computed with the code MATRIZG.f[28] from the optimized geometries. The program BIDIM.f, designed for the study of the ethanol far-IR spectrum,[22] and the subroutines constructed for the study of the overall rotation of acetic acid[23] have been employed for the determination of torsional energy levels and rotational parameters. Integral elements for the top symmetric functions are defined in ref 29.

The Molecular Structure of Glycolaldehyde. Glycolaldehyde exhibits two large amplitude vibrations responsible for the nonrigidity of the molecule: the central C−C bond torsion and the alcoholic hydroxyl torsion. The corresponding independent variables θ_1 and θ_2 can be identified with the O4C2C1O3 and H6O3C1C2 dihedral angles (see Figure 1). The OH torsion can be interpreted as the internal rotation of a top (OH) with respect to a fixed frame (COH−CH_2). In contrast, the C−C torsion represents the internal rotation of two quasi-equivalent tops, COH and CH_2OH, with respect to each other.

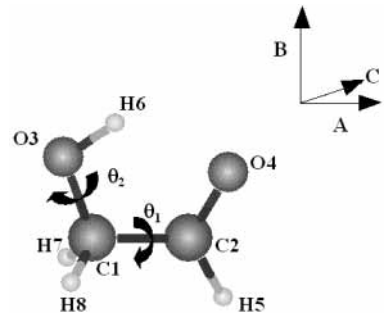

Figure 1. The definition of the θ_1 and θ_2 torsional coordinates and the axis system.

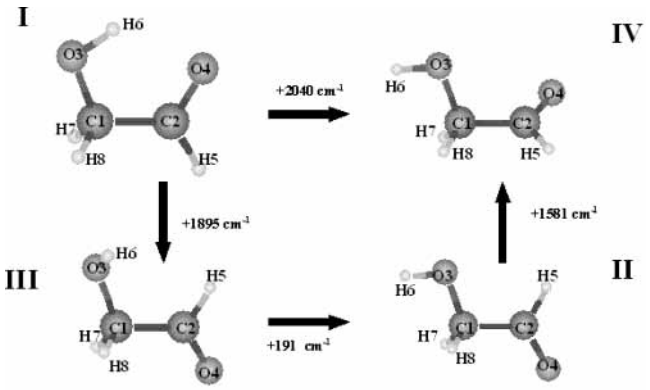

Figure 2. The four conformers of glycolaldehyde. The energies correspond to the one-dimensional barriers that hinder the conformer intertransformation.

If the structure is fully optimized at the MP2/cc-pVQZ level from different starting points, four conformers, I (0,0), II (180,180), III ((197.9,75.8), or (162.1,−75.8)), and IV (0,180), are found (see Figure 2). They are ordered following an increasing energy criterion. Three of them are planar with C_s symmetry, whereas the other one is a double minimum. In this case, the molecular plane is lost for minimizing the nonbonding steric repulsions between hydrogens H5 and H6 (see Figure 1). Hence, the potential energy surface shows a total number of five holes, two cis minima (I and IV) and three trans minima (II, III and III′). The most stable cis geometry (cis-I) is stabilized by the formation of a 2.0661 Å hydrogen bond between the hydroxyl hydrogen and the carbonyl oxygen. It breaks down during the torsions to produce the secondary minima of which the relative energies are higher than 1200 cm^{-1}. Table 1 shows the MP4(SDTQ)/cc-pVQZ relative energies. Conformers II and III lie at 1278.2 and 1297.2 cm^{-1} over the I-cis conformer, whereas the relative energy of the cis-IV is 1865.2 cm^{-1}. The planar geometry (θ_1,θ_2) = (180,180) represents a maximum.

The OH torsion interconverts trans forms (II and III) of similar stabilities (see Figure 3b). Their low energy difference (ΔE-(MP4(SDTQ)/cc-pVQZ) = 19 cm^{-1}) impedes definitive assertion of which one of the two geometries is the most stable. With cc-pVQZ, the most stable form is II, but if calculations are performed with cc-pVTZ, III appears slightly more stable (ΔE = −3.1 cm^{-1}). With the zero point correction and the triple-ζ basis set, the II form presents an energy 59.3 cm^{-1} lower than the one of III, as occurs with QZ. However, it can be asserted that *trans*-glycolaldehyde behaves from the spectroscopic point of view as a methyl group showing internal rotation and a distorted C_{3v} symmetry.[24] The three minima are separated ∼120° by relatively low barriers.

Table 1 shows some characteristic structural and spectroscopic properties. It may be remarked that the cis and trans rotational

TABLE 1: Potential and Kinetic Parameters of Glycolaldehyde Conformers[a]

conformers	I	II	III	IV
symmetry	C_s	C_s	C_1	C_s
E_R (cm^{-1})	0.0[b]	1278.2	1297.2	1865.2
θ_1 (deg)	0.0	180.0	197.9	0.0
θ_2 (deg)	0.0	180.0	75.8	180.0
μ (D)	2.9153	3.3500	2.1146	4.7434
		Kinetic Energy Parameters		
A (MHz)	18 464.6884	38 896.1385	36 917.3315	19 534.1783
B (MHz)	6635.2532	4415.7661	4335.0896	6131.5172
C (MHz)	5032.5810	4066.2187	4082.1320	4805.3460
κ	−0.761 37	−0.979 93	−0.983 76	−0.819 92
B_{11} (cm^{-1})	4.1345	2.8610	2.78416	4.3551
B_{22} (cm^{-1})	22.4992	22.3874	22.5553	22.1783
B_{12} (cm^{-1})	-2.6460	1.0752	-0.1873	−0.7903

Potential Energy Barriers (cm^{-1})					
V(I↔IV)	V(II↔III)	V(III↔III)	V(I↔III)	V(III↔III)	V(II↔IV)
cis ↔ cis	trans ↔ trans	trans ↔ trans	cis ↔ trans	trans ↔ trans	cis ↔ trans
($\theta_1 \propto 0°$)	($\theta_1 \propto 180°$)	($\theta_1 \propto 180°$)	($\theta_2 \propto 0°$)	($\theta_2 \propto 0°$)	($\theta_2 \propto 180°$)
2040	191	713	1895	32	1581
$\theta_2 = 1351$	$\theta_2 = 1251$	$\theta_2 = 01$	$\theta_1 = 791$	$\theta_1 = 1801$	$\theta_1 = 641$
(Figure 3a)	(Figure 3b)	(Figure 3b)	(Figure 3c)	(Figure 3c)	(Figure 3d)

[a] Calculated with MP4(SDTQ)/cc-pVQZ//MP2/cc-pVQZ. [b] $E_a = -228.786\,977$ au.

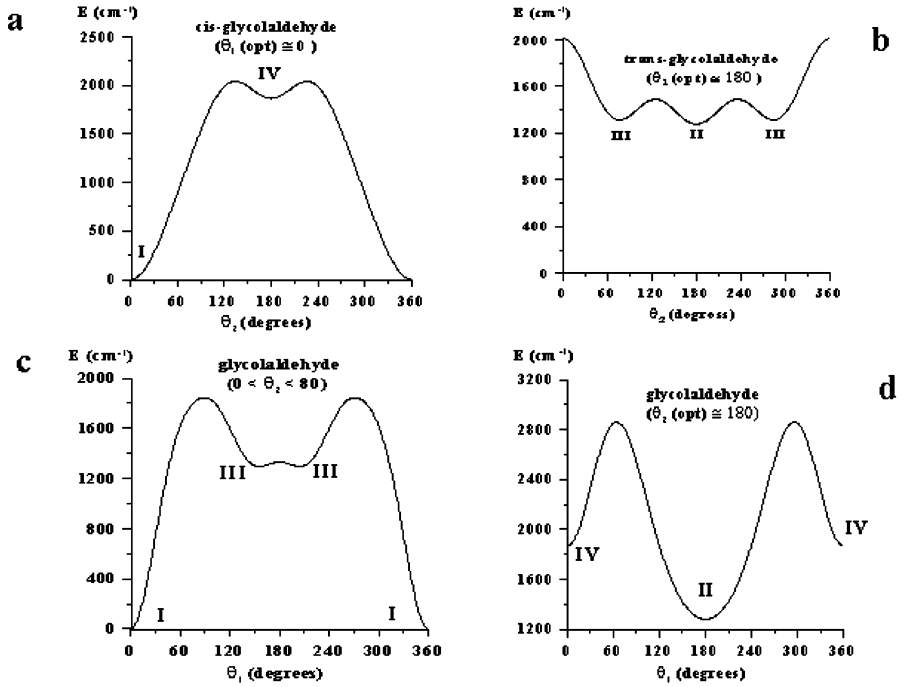

Figure 3. The one-dimensional PES of glycolaldehyde: (a) $V^{CIS}(\theta_2)$ ($\theta_1 \approx 0°$); (b) $V^{TRANS}(\theta_2)$ ($\theta_1 \approx 180°$); (c) $V(\theta_1)$ ($\theta_2 \approx 0°$); (d) $V(\theta_1)$ ($\theta_2 \approx 180°$).

constants are quite different, whereas the OH torsion is basically responsible for the dipole moment variation. The dipole moment is one the few properties of glycolaldehyde available in the literature.[8−9] For the absolute cis minimum, the MP2/cc-pVQZ calculations lead to a dipole moment value of 2.9153 D (μ_a = 0.2682 and μ_b = 2.9029 D), which is higher than the experimental one (μ = 2.33, μ_a = 0.26, and μ_b = 2.33 D) of Marstokk and Møllendal.[9] There is a reasonable agreement between experiments and calculations. Small differences can arise from the failure of the MP2 approximation to describe the electronic distribution between the aldehydic and alcoholic groups. The trans form shows a relatively low dipole moment (2.1146 D).

The two cis conformers are asymmetric tops with rotational constants equal to 18 464.6884, 6635.2532, and 5032.5810 MHz (I-cis) and 19 534.1783, 6131.5172, and 4805.3460 MHz (IV-cis). In principle, these values can be compared with those measured for the cis-I conformer in the zero vibrational energy level (18 446.260 97, 6525.996 543, and 4969.234 992 MHz).[11]

The trans conformers are near-symmetric prolates (κ(II) = −0.979 93; κ(III) = −0.983 76). The corresponding MP2/cc-pVQZ rotational constants are 38 896.1385, 4415.7661, and 4066.2187 MHz for the II-conformer and 36 917.3315, 4335.0896, and 4068.3973 MHz for the III-conformer. Because *trans*-glycolaldehyde has not been detected in the ISM and the corresponding rotational spectrum has not been recorded, the calculated values cannot be compared with experiments. At room temperature, experimental mixtures appear to contain only the cis forms.[8−9] Future experiments are indispensable for starting the refinement of the calculations.

One question that ab initio calculations can answer is whether the thermodynamical properties allow the coexistence of various

conformers in the interstellar medium. At very low temperatures, only the cis levels appear to be populated (the Bolzmann populations of the cis and trans ground states are 0.5311 and 0.0025 at 273.15 K and 1.0 and 0.0 at 10.15 K). From the astrophysical point of view, it is also of interest to discuss the coexistence of the cis and trans conformers on the basis of the internal rotation barriers. It could be possible if the formation processes follow different channels and the rotational barriers are high enough for hindering the trans/cis transformation. In this case, the two conformers can behave as different molecules.

The internal barriers of Table 1 have been calculated from the curves of Figure 3 produced from the fitting of the energies of a set of selected conformations related to different values of one coordinate (θ_1 or θ_2). Energies have been evaluated in one dimension optimizing the remaining $3N - 7$. For this reason, they do not correspond to those employed for the calculation of the two-dimensional potential energy surface where $3N - 8$ coordinates are optimized. Figure 3a represents the cis conformer energy variation with OH. In this case, θ_1 has been allowed to relax. Curve 3b corresponds to the variation of OH in the trans conformer. Curves 3c and 3d are functions of the energy with the central bond torsion. In these cases, θ_2 has been optimized around the equilibrium values corresponding to the conformers I and IV. The cis/trans transformation (I/III) is hindered by barrier of 1895 cm $^{-1}$, whereas the trans/cis transformation (III/I) is hindered by barrier of 598 cm^{-1}. The cis form OH torsion (I-cis/IV-cis) requires it to save an internal rotation barrier of 2040 cm^{-1}, whereas for the trans form the barriers are relatively low (V(II-trans/III-trans) = 191 cm^{-1} and V(III-trans/III′-trans) = 713 cm^{-1}.

The Torsional Energy Levels ($J = 0$). The torsional energy levels are calculated variationally using a flexible model in two dimensions. The two torsional angles are considered independent variables, whereas the remaining $3N - 8$ coordinates are allowed to relax. Therefore, the vibrational effects of the medium and small amplitude modes on the large amplitude modes are partially described. The zero point vibrational correction is added for improving the results.

This flexible model has been tested for many systems using Möller−Plesset theory for the electronic structure.[16−24] Usually, differences between experimental and calculated frequencies are lower than 5 cm^{-1}. It is well-known that it works well if the interactions are small enough but large interactions can introduce numerical errors. The harmonic analysis in $3N - 6$ dimensions allows a first evaluation of the nature of the vibrational modes that may interact strongly. Table 2 shows the harmonic frequencies of the four conformers calculated with MP2/cc-pVTZ and assigned by isotopic substitution. Considering symmetry and energy criteria, it may be expected that the aldehydic hydrogen wagging will be the single mode that can interact significantly with the torsions. It may be anticipated that the vibrational effects of the remaining modes will be well described by the flexible model.[30]

In the case of cis-I, the frequencies for deuterated glycolaldehyde (COH−CO_2D) and the experimental values of ref 10 are also shown in Table 2. With the new information upcoming from the ab initio calculations, four of the nine bands observed in the absorbance spectrum have been reassigned.

The vibrational Hamiltonian for $J = 0$ can be identified with the pure torsional operator:

$$\hat{H} = \hat{H}_T = \hat{H}_{\theta_1} + \hat{H}_{\theta_2} + \hat{H}_{\theta_1,\theta_2}$$

where H_{θ_1} and H_{θ_2} are one-dimensional operators for the central bond and the hydroxyl torsional motions, respectively. H_{θ_1,θ_2} represents the torsion−torsion interaction term. H_T can be written as[22]

$$\hat{H}_T = -\left(\frac{\partial}{\partial\theta_1}\right)B_{11}\left(\frac{\partial}{\partial\theta_1}\right) - \left(\frac{\partial}{\partial\theta_1}\right)B_{12}\left(\frac{\partial}{\partial\theta_2}\right) - \left(\frac{\partial}{\partial\theta_2}\right)B_{12}\left(\frac{\partial}{\partial\theta_1}\right) - \left(\frac{\partial}{\partial\theta_2}\right)B_{22}\left(\frac{\partial}{\partial\theta_2}\right) + V(\theta_1,\theta_2) + V'(\theta_1,\theta_2) + V^{ZPVE}(\theta_1,\theta_2)$$

V represents the potential energy surface, V' is the pseudopotential, and V^{ZPVE} is the zero point vibrational correction; B_{11}, B_{22}, and B_{12} are the central bond torsion, hydroxyl torsion, and torsion−torsion interactions kinetic energy parameters. They are related to the vibrational elements g_{44} and g_{55} and g_{45} of the **G** matrix ($B_{11} = (\hbar^2/2)g_{44}$, $B_{22} = (\hbar^2/2)g_{55}$, and $B_{12} = (\hbar^2/2)g_{45}$; 1 = CC torsion and 2 = OH torsion). The pseudopotential V' can be calculated with the code described in ref 28 from the geometries, but as was observed for acetic acid,[23] its effect on the levels is negligible. It is defined as

$$V' = \frac{1}{4}\sum_{k=1}^{2}\sum_{l=1}^{2}\left[\left(\frac{\partial}{\partial q_k}\right)B_{kl}\left(\frac{\partial \ln g}{\partial q_l}\right) - \left(\frac{\partial \ln g}{\partial q_k}\right)B_{kl}\left(\frac{\partial}{\partial q_l}\right)\right] + \frac{1}{16}\sum_{k=1}^{2}\sum_{l=1}^{2}\left(\frac{\partial \ln g}{\partial q_k}\right)B_{kl}\left(\frac{\partial \ln g}{\partial q_l}\right) \qquad (q_1 = \theta,\ q_2 = \theta_2)$$

The Hamiltonian commutes with the C_s group symmetry operations. The PES, the zero point vibrational correction, and the kinetic parameters B_{11}, B_{22}, and B_{12} are totally symmetric and can be described by fitting the values of each conformation to a periodic function transforming as the A = irreducible representation:

$$F'(\theta_1,\theta_2) = \sum_{N=0}\sum_{L=0}(F_{NL}^{cc}\cos N\theta_1 \cos L\theta_2 + F_{NL}^{ss}\sin N\theta_1 \sin L\theta_2)$$

The potential energy surface (see Figure 4) has been determined by fitting to eq 3 the relative energies of a set of 74 conformations. The energies have been calculated with MP4(SDTQ)/cc-pVQZ, optimizing $3N - 8$ coordinates of each

TABLE 2: Harmonic Frequencies of the Glycolaldehyde Conformers (in cm^{-1}) calculated with MP2/cc-pVTZ

assignment	I (OH)	expt[a] (I)	I (OD)	II	III	IV
	A′		A′	A′		A′
C−C−O bend	293.9		282.2	324.1	333.9	262.5
O=C−C bend	769.9	**751.6**	737.7	548.3	529.0	729.7
C−C stretch	889.8	**860.4**	885.4	1027.1	1056.3	882.9
C−O stretch	1150.2	**1114.6**	1174.6	1113.3	1108.7	1159.9
H−O−C bend	1313.9	**1275.3**	1033.3	1234.6	1220.1	1230.7
O−C−H bend	1405.5		1408.2	1389.0	1350.0	1425.3
H_2C twist	1457.3		1396.8	1447.0	1411.8	1457.4
H−C−H bend	1501.6		1500.6	1506.0	1486.0	1503.1
C=O stretch	1768.6	1754.2	1768.1	1785.7	1778.1	1798.8
C−H stretch	3005.2	2708.2	3005.6	2985.7	2963.3	2938.8
CH_2 stretch	3044.5	2832	3045.0	3055.3	3081.7	3018.2
O−H stretch	3735.5	3548.8	2717.3	3882.3	3864.9	3875.0
	A″		A′	A″		A″
C−C tor	**213.4**		206.8	59.8	78.6	179.6
O−H tor	**425.7**		323.5	222.0	309.9	252.1
H wag	738.2		738.0	747.2	734.3	741.9
CH_2 twist	1117.7		1116.0	1117.6	1086.0	1116.3
H_2C−C bend	1266.4		1263.8	1258.4	1400.2	1273.5
CH_2 stretch	**3081.1**	2881.1	3081.0	3107.2	3142.2	3058.6
ZPVE[b]	13 589.2		13 589.2	13 405.3	13 467.4	13 452.3

[a] From ref 10; some experimental values (in bold) have been reassigned. [b] ZPV (au) = −228.595 772 (I), −228.590 514 (II), −228.590 244 (III), and −228.587 707 (IV).

conformation at the MP2/cc-pVQZ level (see Table 3). Then,

$$V(\theta_1,\theta_2) = 2021.596 - 179.902\cos\theta_2 + 71.983\cos 2\theta_2 + 159.175\cos 3\theta_2 - 4.889\cos 4\theta_2 - 2.334\cos 5\theta_2 + 1.255\cos 6\theta_2 + 164.444\cos\theta_1 - 518.907\cos\theta_1\cos\theta_2 - 185.22\cos\theta_1\cos 2\theta_2 - 32.407\cos\theta_1\cos 3\theta_2 - 7.902\cos\theta_1\cos 4\theta_2 - 0.275\cos\theta_1\cos 5\theta_2 - 0.156\cos\theta_1\cos 6\theta_2 - 561.717\cos 2\theta_1 - 171.206\cos 2\theta_1\cos\theta_2 - 155.729\cos 2\theta_1\cos 2\theta_2 - 60.475\cos 2\theta_1\cos 3\theta_2 - 22.492\cos 2\theta_1\cos 4\theta_2 - 4.914\cos 2\theta_1\cos 5\theta_2 - 0.879\cos 2\theta_1\cos 6\theta_2 - 264.087\cos 3\theta_1 - 56.610\cos 3\theta_1\cos\theta_2 - 43.674\cos 3\theta_1\cos 2\theta_2 - 29.160\cos 3\theta_1\cos 3\theta_2 - 12.339\cos 3\theta_1\cos 4\theta_2 - 5.527\cos 3\theta_1\cos 5\theta_2 - 1.755\cos 3\theta_1\cos 6\theta_2 - 44.948\cos 4\theta_1 - 7.538\cos 4\theta_1\cos\theta_2 - 11.004\cos 4\theta_1\cos 2\theta_2 - 8.506\cos 4\theta_1\cos 3\theta_2 - 8.757\cos 4\theta_1\cos 4\theta_2 - 5.767\cos 4\theta_1\cos 5\theta_2 - 2.383\cos 4\theta_1\cos 6\theta_2 + 7.123\cos 5\theta_1 + 0.669\cos 5\theta_1\cos\theta_2 - 6.164\cos 5\theta_1\cos 2\theta_2 - 3.354\cos 5\theta_1\cos 3\theta_2 - 4.544\cos 5\theta_1\cos 4\theta_2 - 4.259\cos 5\theta_1\cos 5\theta_2 - 2.023\cos 5\theta_1\cos 6\theta_2 + 9.917\cos 6\theta_1 + 1.038\cos 6\theta_1\cos\theta_2 - 0.558\cos 6\theta_1\cos 2\theta_2 - 0.464\cos 6\theta_1\cos 3\theta_2 - 1.397\cos 6\theta_1\cos 4\theta_2 - 1.935\cos 6\theta_1\cos 5\theta_2 - 1.105\cos 6\theta_1\cos 6\theta_2 + 283.393\sin\theta_1\sin\theta_2 + 200.494\sin\theta_1\sin 2\theta_2 + 26.131\sin\theta_1\sin 3\theta_2 + 5.456\sin\theta_1\sin 4\theta_2 - 0.063\sin\theta_1\sin 5\theta_2 + 204.295\sin 2\theta_1\sin\theta_2 + 65.529\sin 2\theta_1\sin 2\theta_2 + 63.903\sin 2\theta_1\sin 3\theta_2 + 22.170\sin 2\theta_1\sin 4\theta_2 + 4.482\sin 2\theta_1\sin 5\theta_2 + 81.231\sin 3\theta_1\sin\theta_2 + 27.936\sin 3\theta_1\sin 2\theta_2 + 26.336\sin 3\theta_1\sin 3\theta_2 + 12.974\sin 3\theta_1\sin 4\theta_2 + 4.866\sin 3\theta_1\sin 5\theta_2 + 9.892\sin 4\theta_1\sin\theta_2 + 13.948\sin 4\theta_1\sin 2\theta_2 + 10.175\sin 4\theta_1\sin 3\theta_2 + 8.778\sin 4\theta_1\sin 4\theta_2 + 3.982\sin 4\theta_1\sin 5\theta_2 - 1.130\sin 5\theta_1\sin\theta_2 + 12.511\sin 5\theta_1\sin 2\theta_2 + 2.865\sin 5\theta_1\sin 3\theta_2 + 3.318\sin 5\theta_1\sin 4\theta_2 + 2.053\sin 5\theta_1\sin 5\theta_2$$

The optimization of the geometry produces deformations in the molecule that can generate unexpected weights in the terms of the fitted potential.[24] This problem can be minimized by frozen linear combination of coordinates during the relaxation process to give a more realistic definition of the independent variables. This refinement of the method is necessary when the deformation has an important effect on the torsional frequencies. In glycolaldehyde, it is difficult to evaluate this effect without comparing the results with experimental data.

The method for calculating the B_{ij} parameters from each optimized geometry is described in ref 28. The ZPVE correction is determined for each conformation within the harmonic approximation with the equation

$$E^{\mathrm{ZPVE}} = \sum_{i=3}^{3N-6} \frac{1}{2}\omega_i$$

TABLE 3: Relative Electronic Energies (in cm^{-1}) of the Selected Conformation of Glycolaldehyde

θ_1	θ_2	E_R	θ_1	θ_2	E_R	θ_1	θ_2	E_R
0	0[a]	0.0	180	0	2012.2			
0	30	419.5	180	30	1785.1			
0	60	1018.0	180	60	1406.5			
0	90	1607.4	180	90	1364.3			
0	120	2025.2	180	120	1503.0			
0	150	1991.2	180	150	1400.5			
0	180	1865.2	180	180	1278.2			
30	0	1125.4	60	0	2722.2	90	0	2949.9
30	30	1723.5	60	30	2934.0	90	30	2875.6
30	60	1994.7	60	60	2808.1	90	60	2535.2
30	90	2342.5	60	90	2941.6	90	90	2516.0
30	120	2645.5	60	120	3168.8	90	120	2649.1
30	150	2535.5	60	150	3064.6	90	150	2590.1
30	180	2326.8	60	180	2888.5	90	180	2563.7
30	−30	663.9	60	−30	2004.6	90	−30	2358.8
30	−60	1035.6	60	−60	1751.2	90	−60	1854.2
30	−90	1710.4	60	−90	2248.2	90	−90	2125.1
30	−120	2237.5	60	−120	2784.0	90	−120	2623.7
30	−150	2333.0	60	−150	2900.5	90	−150	2699.9
120	0	2488.8	150	0	2108.9			
120	30	2290.8	150	30	1905.0			
120	60	1934.9	150	60	1575.9			
120	90	1882.5	150	90	1511.5			
120	120	1966.3	150	120	1579.8			
120	150	1903.5	150	150	1477.6			
120	180	1903.4	150	180	1423.8			
120	−30	2080.1	150	−30	1818.9			
120	−60	1574.2	150	−60	1379.9			
120	−90	1678.0	150	−90	1394.5			
120	−120	2048.8	150	−120	1643.2			
120	−150	2068.2	150	−150	1586.1			

[a] $E_a = -228.786\,977$ au.

where the summation is extended to all the vibrations once the torsional modes are eliminated. The harmonic fundamentals are obtained with MP2/cc-pVTZ at different points of the surface.

The levels are calculated using as a trial function a symmetry-adapted double Fourier series. Once the matrix is diagonalized, the most arduous effort is constrained by the classification of the levels due the proximity of the two modes and the small gaps between splittings. For this purpose, four criteria are considered: (1) the symmetry; (2) the values of the probability integrals around the minima,

$$\int_{\theta_1=p}^{\theta_2=q}\int_{\theta_2=p'}^{\theta_2=q'} \psi_T^*\psi_T \,\mathrm{d}\theta_1\,\mathrm{d}\theta_2$$

that allow one to distinguish between cis and trans levels; (3) the expectation values of the one-dimensional operators in the torsional levels,

$$\langle H_i\rangle = \langle\psi_T|H_i|\psi_T\rangle = \left\langle\psi_T\left|B_i^0\frac{\partial^2}{\partial i^2} + V(i,0)\right|\psi_T\right\rangle \qquad i = \theta_1,\theta_2$$

that allow one to assign the levels to each torsional mode; (4) the intensities of the infrared transitions that allow one to construct sequences of the levels.

In Table 4, the energies calculated with and without the zero vibrational correction are compared. As we demonstrated in a previous paper testing different high-level corrections (extrapolation of the basis set, core correlation, adiabatic corrections, etc.) in the current model, the consideration of the zero point vibrational energy is relevant for determining accurate excitations.[25] For the cis conformer, the fundamental frequency of the CC torsion has been determined to be 202.1 cm^{-1} (without ZPVE) and to be 199.3 cm^{-1} (with ZPVE), below the harmonic frequency of Table 2 (213.4 cm^{-1}). The effect of the vibrational

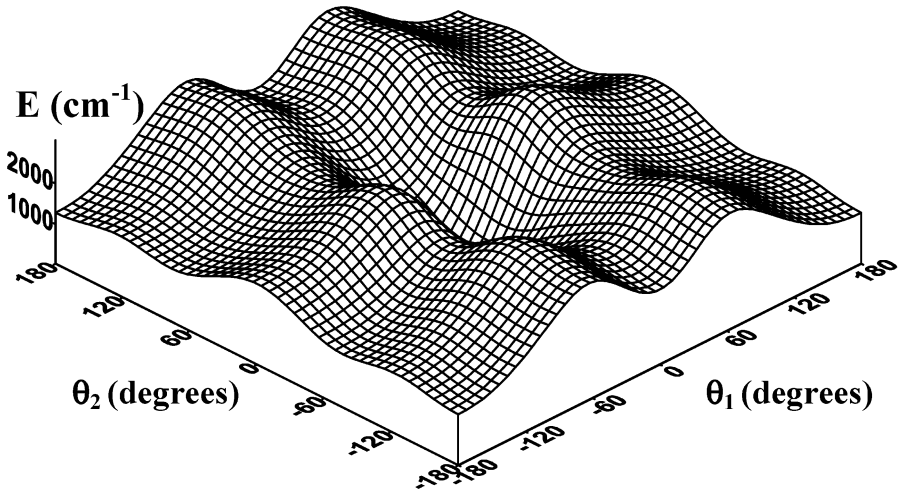

Figure 4. The two-dimensional potential energy surface of glycolaldehyde.

TABLE 4: Torsional Energy Levels of COH−CH_2OH (OH) and COH−CH_2OD (OD) (in cm^{-1})

		cis-OH		cis-OD			trans-OH	trans-OD
		−ZPVE	+ZPVE	−ZPVE			−ZPVE	−ZPVE
0 0	A′	0.0	0.0	0.0	0 0	A′	1111.6	1138.1
					$0\,0^-$	A″	1161.2	1180.5
					$0\,0^+$	A′	1165.0	1180.8
1 0	**A″**	**202.1**	**199.3**	**194.5**	**1 0**	A″	1183.5	1210.8
2 0	A′	393.5	392.7	376.4	$1\,0^-$	A″	1221.3	1238.4
3 0	A″	578.0	582.8	552.6	$1\,0^+$	A′	1223.3	1240.4
4 0	A′	756.2	768.7	725.0				
5 0	A″	927.9	948.9	892.7	2 0	A′	1258.5	1286.7
6 0	A′	1091.3	1122.1	1054.6	$2\,0^+$	A′	1282.6	1298.4
7 0	A″	1246.4	1286.6	1209.1	$2\,0^-$	A″	1290.6	1301.7
8 0	A′	1389.6	1442.5	1355.0				
					3 0	A″	1333.4	1365.7
0 1	**A″**	**352.1**	**368.7**	**279.8**	$3\,0^+$	A″	1347.5	1359.0
0 2	A′	657.4	687.1	540.0	$3\,0^-$	A′	1355.8	1364.0
0 3	A″	924.1	964.5	784.5				
0 4	A′	1164.6	1214.3	1016.3	4 0	A′	1418.6	1404.6
0 5	A″	1387.0	1446.7	1237.3	$4\,0^+$	A′	1403.4	1427.6
					$4\,0^-$	A″	1409.7	1420.8
1 1	A′	547.1	558.5	463.5				
2 1	A″	736.7	750.1	634.8				
1 2	A″	845.5	866.9	710.7	**0 1**	A″	1274.7	1264.9
3 1	A′	921.5	940.7	802.5	$0\,1^+$	A′	1363.3	1327.8
2 2	A′	1032.7	1057.3	868.5	$0\,1^-$	A″	1399.1	1352.0
1 3	A’	1104.3	1131.7	942.1				
4 1	A″	1100.0	1126.7	967.8				
3 2	A″	1216.7	1248.8	1023.9	**1 1**	A′	1338.1	1333.9
2 3	A″	1287.1	1319.5	1087.5	$1\,1^+$	A″	1431.7	1395.5
					$1\,1^-$	A′	1456.4	1393.6
			One Dimension					
	1 0		218.4				218.5	
	0 1		283.4				276.7	

corrections is more important for the OH torsion where the fundamental varies from 352.1 cm^{-1} (without ZPVE) to 368.7 cm^{-1} (with ZPVE). Also, the anharmonicity is more important for OH (υ = 368.7 cm^{-1} and ω = 425.7 cm^{-1}). For the deuterated species, the two fundamentals have been determined to be 194.5 and 279.8 cm^{-1}, whereas the harmonic values of Table 2 are 206.8 and 323.5 cm^{-1}.

Calculations have been also performed in one dimension for evaluating the torsional interactions. In this case, the Hamiltonian is determined from the energies and geometries obtained by optimizing $3N - 7$ internal coordinates. By comparing the two-dimensional results (202.1 and 352.1 cm^{-1}) with those obtained in one dimension (218.4 and 283.4 cm^{-1}), it may be inferred that the effect on the OH torsion is larger than that on the central bond torsion. As was first observed for ethanol,[22] the one-dimensional model is quite nonsensical in the case of the OH torsion. For the trans levels, the interactions between the two modes are really significant.

The labeling of the trans levels has been particularly arduous. Around the trans minima, the potential is quite anharmonic and

TABLE 5: Predicted Far-IR Frequencies (cm^{-1}) and Absolute Intensities for Cis and Trans Glycolaldehyde Calculated at 273.15 K

		cis				trans		
$\upsilon\upsilon \rightarrow \upsilon'\upsilon'$	sym	freq	int	ω	$\upsilon\upsilon \rightarrow \upsilon'\upsilon'$	freq	int	ω
			CC Transitions					
$00 \rightarrow 10$	$A_1 \rightarrow A_2$	199.2	0.0038	213.4	$00 \rightarrow 10$	72.0	0.4×10^{-4}	59.8
$10 \rightarrow 20$	$A_2 \rightarrow A_1$	193.5	0.0031			56.2	0.4×10^{-5}	78.6
$20 \rightarrow 30$	$A_1 \rightarrow A_2$	190.1	0.0016			62.1	0.1×10^{-4}	78.6
$30 \rightarrow 40$	$A_2 \rightarrow A_1$	185.9	0.0009		$10 \rightarrow 20$	74.9	0.6×10^{-4}	
$40 \rightarrow 50$	$A_1 \rightarrow A_2$	180.2	0.0003			61.3	0.1×10^{-4}	
						67.3	0.3×10^{-4}	
			OH Transitions					
$00 \rightarrow 01$	$A_1 \rightarrow A_2$	368.7	0.1022	425.7	$00 \rightarrow 01$	163.2	0.8×10^{-4}	222.0
$01 \rightarrow 02$	$A_2 \rightarrow A_1$	318.4	0.0249			234.1	0.8×10^{5}	309.9
$02 \rightarrow 03$	$A_1 \rightarrow A_2$	277.4	0.0054			202.1	0.4×10^{-5}	309.9
$03 \rightarrow 04$	$A_2 \rightarrow A_1$	249.7	0.0012					
$04 \rightarrow 05$	$A_1 \rightarrow A_2$	232.4	0.0003					
			Combination Bands					
$01 \rightarrow 11$	$A_2 \rightarrow A_1$	189.8	0.0017					
$10 \rightarrow 11$	$A_2 \rightarrow A_1$	359.2	0.0356					
$11 \rightarrow 21$	$A_1 \rightarrow A_2$	191.6	0.0012					
$11 \rightarrow 12$	$A_1 \rightarrow A_2$	308.4	0.0087					

TABLE 6: Rotational Levels (cm^{-1}) for the Cis and the Trans Vibrational Ground States ($\upsilon\upsilon'$) = (0 0) and the First Cis Excited State ($\upsilon\upsilon'$) = (1 0)

			(0,0)			(1,0)
J	$\lvert K_a \rvert$	$\lvert K_c \rvert$	symm	cis	trans	symm	cis
0	0	0	A′	0.000	1111.573	A″	202.100
1	0	1	A″	0.386	1111.856	A′	202.484
1	1	1	A″	0.787	1112.988	A′	202.888
1	1	0	A′	0.839	1112.977	A″	202.938
2	0	2	A′	1.153	1112.422	A″	203.248
2	1	2	A′	1.507	1113.565	A″	203.605
2	1	1	A″	1.663	1113.532	A′	203.767
2	2	1	A″	2.866	1116.926	A″	204.973
2	2	0	A′	2.870	1116.926	A′	204.968
3	0	3	A″	2.293	1113.271	A′	204.383
3	1	3	A″	2.585	1114.434	A′	204.679
3	1	2	A′	2.896	1114.368	A″	204.983
3	2	2	A′	4.024	1117.790	A″	206.121
3	2	1	A″	4.047	1117.790	A′	206.144
3	3	1	A″	6.161	1123.437	A′	208.269
3	3	0	A′	6.161	1123.437	A″	208.269

TABLE 7: Computed Rotational Parameters for *cis*- and *trans*-CH_2OHCOH at the Lowest Vibrational States

	cis					trans	
	ground state (0,0)			first excited state (1,0)		ground state (0.0)	
	expected values	fitted values	exptl values[11]	fitted values	exptl values[8]	expected values	fitted values
A (MHz)	18 537.1	18 583.85	18 446.260 97	18 620.65	18 463.653	38 387.4	38 019.19
B (MHz)	6566.5	6563.83	6525.996 543	6518.27	6482.563	4405.8	4406.79
C (MHz)	5008.0	5009.34	4969.234 992	4998.43	4965.085	4073.2	4076.73
D_J (kHz)		−20.18	6.222 193 1	−74.34	−25.58		−109.28
D_{JK} (kHz)		−82.36	−20.395 79	35.50	−72.46		605.67
D_K (kHz)		138.38	47.722 86	−2.26	95.0		4491.06
δ_J (kHz)		48.17	1.834 147	7.23	5.309		
δ_K (kHz)		−5.53	8.874 43	−5.14	−3.80		

the separation between splittings is larger than the gaps of the levels. The shape of the one-dimensional potential energy surface for the OH torsion (see Figure 3b) is similar to the one describing the internal rotation of a methyl group. There are three quasi-equivalent holes separated by barriers of 191 and 713 cm^{-1}. Each level splits into three components with a relatively high energy difference as a consequence of the low barriers. The zero vibrational energy has been calculated to be 1111.6, 1161.2, and 1165.0 cm^{-1}. The two fundamentals have been calculated to be 72.0, 56.2, and 62.1 cm^{-1} and 163.2, 234.1, and 202.1 cm^{-1}, whereas the energy differences between splittings are 49.6 and 54.4 cm^{-1}.

Infrared intensities are quite useful in the classification of the levels using the large difference between the oscillator strengths for the two modes. The intensities of the Q branches of the "out of plane" type C bands are calculated with the equation[16]

$$I = \frac{q}{3R^2e^2B}\omega(P_jP_i)\langle\psi_i|\mu_c|\psi_j\rangle^2$$

where i and j represent two connected states. R is the average radius of the rotor (1.39 Å), $B = (B_{11}B_{22})^{1/2}$, μ_c are the dipole moment components that transform as the A″ representation, and P_K represents the Bolzmann population; ω is the frequency and q the nuclear statistical weight. The selection rules are shown in Appendix I.

The $\boldsymbol{\mu_c(\theta_1,\theta_2)}$ moment has been calculated with MP2/cc-pVQZ for each conformation and fitted to an adapted Fourier series of A″ symmetry. Table 5 shows frequencies and intensities of three series of transitions of the far-infrared spectrum calculated at 273.15 K. The strongest band corresponds to the OH torsion fundamental 0,0 → 0,1 (frequency = 368.7 cm^{-1}; intensity = 0.1022). The central bond torsion fundamental shows an intensity of 0.0038. In the case of the trans minimum, the OH fundamental (163.2 cm^{-1}) is also the most intense band (0.8×10^{-4}).

The Rotational Parameters of Glycolaldehyde. For $J \neq 0$, the rotational−torsional Hamiltonian is written as the sum of the pure rotational Hamiltonian and the interaction operators,

$$H = H_{ROT} + H_{TR}$$

defined by the equations[29]

$$\hat{H}_R = \sum_{\lambda=1}^{3}\sum_{\mu=1}^{3} g_{\lambda\mu}P_\lambda P_\mu \qquad \lambda,\mu = x,y,z$$

$$\hat{H}_{RT} = \frac{i}{2}\sum_{\lambda=1}^{3}\left(2g_{\lambda4}(\theta_1)P_\lambda\frac{\partial}{\partial\theta_1}\left(\partial\frac{g_{\lambda4}}{\partial\theta_1}\right)\frac{\partial}{\partial\lambda} + 2g_{\lambda5}(\alpha)P_\lambda\frac{\partial}{\partial\theta_2}\left(\partial\frac{g_{\lambda5}}{\partial\theta_2}\right)\frac{\partial}{\partial\lambda}\right)$$

where x, y, and z are the molecular Cartesian axis. P_λ represents the angular momentum components, and $g_{\lambda\mu}$ and $g_{\lambda n}$ are the rotational and rotational−torsional elements of the **G** matrix.[28] The definition of the molecular axis follows the PAM method (see Figure 1). In I-cis, the A molecular axis is almost to the C−C central bond, B lies in the cis plane, and C lies in the trans plane (see Figure 1). Then, the g_{ij} elements for ij = 11, 22, 33, 12, 14, 24, 15, and 25 transform as A′ and those for ij = 13, 23, 34, and 35 transform as A″. The totally symmetric elements can be fitted to a function formally identical to the one of the potential. For the asymmetric elements, the analytic form is

$$F''(\theta,\alpha) = \sum_{N=0}\sum_{L=0}(F_{NL}^{cs}\cos N\theta_1 \sin L\theta_2 + F_{NL}^{sc}\sin N\theta_1 \cos)$$

The rotational−vibrational energy levels are calculated variationally using contrated basis set to reduce the Hamiltonian matrix dimension that increases with the J rotational quantum number. It has to be taken into consideration that for glycolaldehyde the convergence of the torsional levels requires two Hamiltonian matrix with dimensions of 1301 (A′) and 1300 (A″).

The contracted basis set for $J \neq 0$ may be a product of solutions of the vibrational Hamiltonian, φ^{TOR}, for describing the torsion, and solutions of the symmetric top for the overall rotation. The set of contract functions, φ^{TOR}, helps the assignments of the rotational energies to the vibrational levels. Then, the complete trial function is

$$\Psi(\theta,\Theta,\phi,\theta_1,\theta_2) = \sum_{n,J,K,M} C_{n,J,K,M}\phi_n^{TOR}(\theta_1,\theta_2)G_{J,\pm K,M}(\Theta,\phi,\chi)$$

where Θ, φ, and κ are the Euler angles. To obtain a real Hamiltonian matrix, the $G_{J,\pm K,M}$ symmetric top solutions are defined in Cartesian coordinates using the linear combinations:

$$G_{J,\pm K,M}(\Theta,\phi,\chi) = B(S_{J+K,M}(\Theta,\phi,\chi)\, e^{i(+K)\chi} \pm (S_{J,K,M}(\Theta,\phi,\chi)\, e^{i(K)\chi})\, e^{iM\phi})$$

where the S functions are symmetric top solutions in spheric coordinates and the sign before the rotational quantum number K corresponds to the sign of the linear combination.

Taking into consideration the symmetry (see Appendix I), the Hamiltonian matrix factorizes in two boxes corresponding to the A′ and A″ representations.

Table 6 shows the rotational levels corresponding to the vibrational cis and trans ground states. They have been calculated using set of 19 cis torsional functions (10 A′ and 9 A″) and 17 trans torsional functions (9 A′ and 8 A″). The levels are labeled with the J, K_a, and K_c rotational numbers. In the case of the cis form, calculations have been performed with the ZPVE correction, although its effect is negligible. By fitting

the energies and the expectations values of the rotational Hamiltonian operators at the levels to the equation

$$E = \langle\psi_i|H_{\mathrm{ROT}}|\psi_i\rangle = +\frac{1}{2}(B+C)J(J+1) + \left[A - \frac{1}{2}(B+C)\right]\langle\psi_i|\hat{J}_z^{\,2}|\psi_i\rangle - D_J[J(J+1)]^2 - D_{JK}J(J+1)\langle\psi_i|J_z^{\,2}|\psi_i\rangle - D_K\langle\psi_i|\hat{J}_z^{\,4}|\psi_i\rangle + H_J[J(J+1)]^3 + H_{JK}[J(J+1)]^2\langle\psi_i|\hat{J}_z^{\,2}|\psi_i\rangle + H_{KJ}J(J+1)\langle\psi_i|\hat{J}_z^{\,4}|\psi_i\rangle + H_K\langle\psi_i|\hat{J}_z^{\,6}|\psi_i\rangle + \frac{1}{4}(B-C)\langle\psi_i|\hat{J}_+^{\,2} + \hat{J}_-^{\,2}|\psi_i\rangle + \delta_J J(J+1)\langle\psi_i|\hat{J}_+^{\,2} + \hat{J}_-^{\,2}|\psi_i\rangle + \delta_K\langle\psi_i|\hat{J}_+^{\,4} + \hat{J}_-^{\,4}|\psi_i\rangle + \phi_J[J(J+1)]^2\langle\psi_i|\hat{J}_+^{\,2} + \hat{J}_-^{\,2}|\psi_i\rangle + \phi_{JK}J(J+1)\langle\psi_i|\hat{J}_+^{\,4} + \hat{J}_-^{\,4}|\psi_i\rangle + \phi_K\langle\psi_i|\hat{J}_+^{\,6} + \hat{J}_-^{\,6}|\psi_i\rangle$$

one is able to evaluate the rotational constants and the centrifugal distortions constants at the levels. This method produces observable parameters and represents an improvement of the usual way consisting in the direct determination of the parameters from ab initio force fields. That method gives unobservable results calculated in the potential minimum.

Table 7 shows the fitted parameters corresponding to three different vibrational states. For the cis conformer, the parameters of the ground state and the first excited state are compared with the experimental values of refs 11 and 8, respectively. For the trans conformers, the tabulated values represent a first prediction.

Acknowledgment. This work has been also supported by the Ministerio de Ciencia y Tecnología of Spain, Grant AYA2002-02117.

Appendix I

Selection rules for the infrared transitions:

A-type bands $\mu_a(A')$	B-type bands $\mu_b(A')$	C-type bands $\mu_c(A'')$
$A' \leftrightarrow A'$	$A' \leftrightarrow A'$	$A' \leftrightarrow A''$
$A'' \leftrightarrow A''$	$A'' \leftrightarrow A''$	

Eigenfunctions for glycolaldehyde:

	φ_T	J	K
A′	$\sum(A_i \cos\theta_1 \cos\theta_2 + B_i \sin\theta_1 \sin\theta_2)$	even	even
	$\sum(A_i \cos\theta_1 \sin\theta_2 + B_i \sin\theta_1 \cos\theta_2)$	even	odd
	$\sum(A_i \cos\theta_1 \cos\theta_2 + B_i \sin\theta_1 \sin\theta_2)$	odd	odd
	$\sum(A_i \cos\theta_1 \sin\theta_2 + B_i \sin\theta_1 \cos\theta_2)$	odd	even
A″	$\sum(A_i \cos\theta_1 \cos\theta_2 + B_i \sin\theta_1 \sin\theta_2)$	even	odd
	$\sum(A_i \cos\theta_1 \sin\theta_2 + B_i \sin\theta_1 \cos\theta_2)$	even	even
	$\sum(A_i \cos\theta_1 \cos\theta_2 + B_i \sin\theta_1 \sin\theta_2)$	odd	even
	$\sum(A_i \cos\theta_1 \sin\theta_2 + B_i \sin\theta_1 \cos\theta_2)$	odd	odd

References and Notes

(1) Hollis, J. M.; Lovas, F. J.; Jewell, P. R. *Astrophys. J.* **2000**, *540*, L107.
(2) Bacher, G.; Tyndall, G. S.; Orlando, L. J. *J. Atmos. Chem.* **2001**, *39*, 171.
(3) Dickens, J. E.; Irvine, W. M.; Nummelin, A.; Møllendal, H.; Saito, S.; Thorwirth, S.; Hjalmarson, A.; Ohishi, M. *Spectrochim. Acta, Part A* **2001**, *57A*, 643.
(4) Hollis, J. M.; Vogel, S. N.; Snyder, L. E.; Jewell, P. R.; Lovas, F. J. *Astrophys. J.* **2001**, *554*, L81.
(5) Huntress, W. T., Jr.; Mitchell, G. F. *Astrophys. J.* **1979**, *231*, 456.
(6) Kaiser, R. I. *Chem. Rev.* **2002**, *102* (5), 1309.
(7) Sorrell, W. H. *Astrophys. J.* **2001**, *555*, L129.
(8) Markstokk, K. M.; Møllendal, H. *J. Mol. Struct.* **1970**, *5*, 205.
(9) Markstokk, K. M.; Møllendal, H. *J. Mol. Struct.* **1973**, *16*, 259.
(10) Niki, H.; Maker, P. D.; Savage, C. M.; Breitenbach, L. P. *Chem. Phys. Lett.* **1981**, *80*, 499.
(11) Butler, R. A. H.; de Lucia, F. C.; Petkie, D. T.; Møllendal, H.; Horn, A.; Herbst, E. *Astrophys. J.* **2001**, *134*, 319.
(12) Crovisier, J. *BASEMOLE*.
(13) Markham, D. G.; Bock, C. L.; Trachtman, M.; Bock C. W. *J. Mol. Struct. (TEOCHEM)* **1999**, *459*, 187.
(14) Su, C. C.; Lin, C. K.; Wu, C. C.; Lien, M. H. *J. Phys. Chem. A* **1999**, *103* (17), 3289.
(15) Chen, C.; Hsu, F. S. *J. Mol. Struct. (THEOCHEM)* **2000**, *506*, 147.
(16) Smeyers, Y. G.; Senent, M. L.; Botella, V.; Moule, D. C. *J. Chem. Phys*, **1993**, *98* (4), 2754.
(17) Senent, M. L.; Moule, D. C.; Smeyers, Y. G. *J. Chem. Phys.* **1995**, *102*, 5952.
(18) Smeyers, Y. G., Villa, M.; Senent, M. L. *J. Mol. Spectrosc.* **1998**, *191*, 232.
(19) Makarewicz, J.; Kreglewski, M.; Senent, M. L. *J. Mol. Spectrosc.* **1997**, *186*, 162.
(20) Muñoz-Caro, C.; Niño, A.; Senent, M. L. *Chem. Phys. Lett.* **1997**, *273*, 135.
(21) Senent, M. L.; Fernández-Herrera, S.; Smeyers, Y. G. *Spectrochim. Acta, Part A* **2000**, *56A*, 1457.
(22) Senent, M. L.; Smeyers, Y. G.; Dominguez-Gómez, R.; Villa, M. *J. Chem. Phys.* **2000**, *112*, 5809.
(23) Senent, M. L. *Mol. Phys.* **2001**, *15*, 1311.
(24) Szalay, V.; Császár, A. G.; Senent, M. L. *J. Chem. Phys.* **2002**, *117*, 6489.
(25) Császár, A. G.; Szalay, V.; Senent, M. L. *J. Chem. Phys.* **2004**, *120* (3), 1203.
(26) Talón, C.; Ramos, M. A.; Vieira, S.; Cuello, G. J.; Bermejo, F. J.; Criado, A.; Senent, M. L.; Bennington, S. M.; Fischer, H. E.; Schober, H. *Phys. Rev. B* **1998**, *58*, 745.
(27) Frisch, M. J.; Trucks, G. W.; Schlegel, H. B.; Scuseria, G. E.; Robb, M. A.; Cheeseman, J. R.; Zakrzewski, V. G.; Montgomery, J. A., Jr.; Stratmann, R. E.; Burant, J. C.; Dapprich, S.; Millam, J. M.; Daniels, A. D.; Kudin, K. N.; Strain, M. C.; Farkas, O.; Tomasi, J.; Barone, V.; Cossi, M.; Cammi, R.; Mennucci, B.; Pomelli, C.; Adamo, C.; Clifford, S.; Ochterski, J.; Petersson, G. A.; Ayala, P. Y.; Cui, Q.; Morokuma, K.; Malick, D. K.; Rabuck, A. D.; Raghavachari, K.; Foresman, J. B.; Cioslowski, J.; Ortiz, J. V.; Stefanov, B. B.; Liu, G.; Liashenko, A.; Piskorz, P.; Komaromi, I.; Gomperts, R.; Martin, R. L.; Fox, D. J.; Keith, T.; Al-Laham, M. A.; Peng, C. Y.; Nanayakkara, A.; Gonzalez, C.; Challacombe, M.; Gill, P. M. W.; Johnson, B. G.; Chen, W.; Wong, M. W.; Andres, J. L.; Head-Gordon, M.; Replogle, E. S.; Pople, J. A. *Gaussian 98*, revision A.1x; Gaussian, Inc.: Pittsburgh, PA, 1998.
(28) Senent, M. L. *Chem. Phys. Lett.* **1998**, *296*, 299.
(29) Senent, M. L. *J. Mol. Spectrosc.* **1998**, *191*, 265.
(30) Senent, M. L.; Fernández-Herrera, S.; Smeyers, Y. G.; Domínguez-Gómez, R. M.; Villa, M. *Mol. Phys.* **1999**, *96*, 775.